Photoinduced Phenomena in Non-metallic Amorphous Materials

Keiji Tanaka

Department of Applied Physics, Graduate School of Engineering, Hokkaido University, Sapporo 060-8628, Japan

E-mail: keiji@eng.hokudai.ac.jp

Photoinduced phenomena in non-crystalline insulators and semiconductors, specifically oxide and chalcogenide glasses, are briefly reviewed with some comments.

1. Introduction

Photoinduced or photosensitive phenomena are widespread in the world. Well-known examples are photosynthesis and heliotropism in plants. Our eyes detect photons through efficient photo-electro-ionic processes. And, there are genetic ideas that the conversion of organic molecules to life embryos is also a kind of photo-stimulated processes[1]. On the other hand, inanimate matters exhibit relatively simpler photoinduced processes, although many mechanisms being still unclear[2]. Examples are photographic reaction in Ag-halide crystals and photo-polymerization in organic resist films, the latter being indispensable for producing semiconductor integrated circuits.

We here note that in general the photoinduced process appears more prominently in non-crystalline solids than that in crystalline solids[3,4]. For instance, Vonwiller mentioned, already in 1919, a marked difference in photoinduced fluidity in amorphous (a-) and crystalline Se[5]. Primak demonstrated that neutron-induced volume changes for vitreous and crystalline SiO_2 are different by one order in time constant[6]. It was also reported that remarkable differences exist in glassy and crystalline chalcogenides for, e.g., photodarkening in As_2S_3[7] and photodoping in Ag/As_2S_3[8]. How can we understand these differences?

Since these materials in crystalline and glassy forms are not very different in optical bandgap energies[7-9], a disordered structure must be responsible for these different behaviors. That is, photo-electronic excitations are similar, while electro-structural processes must be different, which can be attributed to the disordered structure in two respects. One is that the *localization* of photo-excited electrons, including holes and electron-hole pairs, which must be indispensable for triggering strong electron-atom interaction. In fact, I am skeptical if some photoinduced phenomenon appears in an ideal crystal at ~0 K, in which photo-excited carriers will spatially extend and no motive forces of electron-atom interaction may exist. The other is that the disordered structure is, in general, less-dense (~10 %) and more *flexible*, and accordingly, it is likely to undergo strong lattice distortions.

In this work, I will present a brief review on photoinduced phenomena in amorphous insulators and semiconductors. Specifically, oxide and chalcogenide glasses having simple compositions such as Se, $Si(Ge)O(S,Se)_2$, and $As_2S(Se,Te)_3$ are comparatively studied, since these materials can be treated in a unified way as the group VIb glass[9]. Amorphous hydrogenated Si (a-Si:H) is also touched for comparison. Related subjects are reviewed recently[3,4,10-12], which should be also referred to. Here, it is just mentioned that studies on photoinduced phenomena in halide glasses are very limited[13]. However, the photographic reaction in Ag-halide crystals may suggest that photoinduced Ag migration in chalco-halide glasses[14] will be an interesting subject.

To make this article in proper length, we will exclude the following three topics. First, particle-irradiation effects induced by neutrons, electrons, and ions are not described. In short, these particles can provide elec-

tronic excitations in similar ways to those by photons, while the particle may add other effects of momentum, charge, and atomic doping[2]. Second, thermo-mechanical shaping using CO_2 lasers etc. may not be regarded as a photoinduced process, since IR light directly excites vibrational modes. Accordingly, the topic is excluded. Third, dopant-related photoinduced phenomena[15,16] are little touched. The dopant can play important roles in oxide glasses by producing mid-gap states, since network formers have wide optical gaps of 5 - 10 eV (Fig. 1). For instance, heavy metallic atoms (Pb, Bi, etc.), transition-metal (Fe, Ni, Mn, Cr, etc.) ions, and rare-earth (Eu, Ce, etc.) ions add sensitive photoinduced phenomena, which are practically promising to some applications such as hole burning memories. Moreover, larger-scale dopants such as metallic clusters and colloidal particles provide a lot of varieties.

2. Fundamentals

Fig. 1 classifies simple non-metallic amorphous materials by optical bandgap energy E_g and structural network dimension. The latter concept[17] may be still controversial, while it can give intuitive views of chain structures in polyethylene and Se, layer structures in $As_2S(Se)_3$ and $GeS(Se)_2$, and three-dimensional networks in $Si(Ge)O_2$ and a-Si(:H)[18].

Among these solids, the oxide (O) and the chalcogenide (S, Se, Te) glass have some common features[9]. All these atoms, belonging to group VIb in the periodic table, have the same outer electronic configuration of

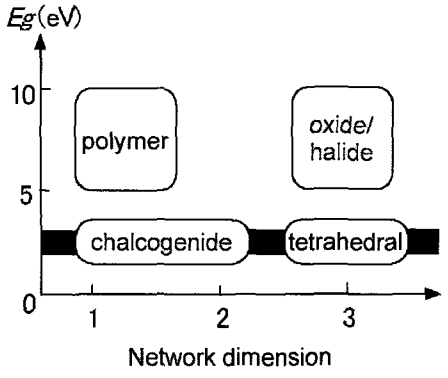

Fig. 1. Classification of amorphous insulators and semiconductors by optical bandgap energy E_g and structural network dimension. The horizontal band represents the photon energy (2 - 3 eV) of visible light.

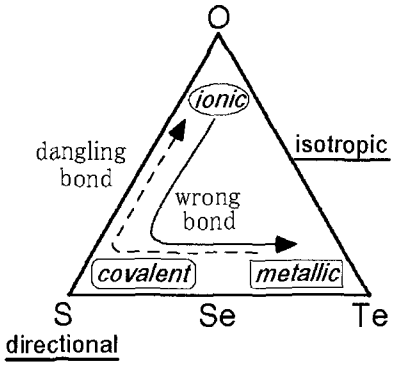

Fig. 2. A unified view of group VIb glasses[9]. Wrong bonds increase and dangling bonds decrease in a sequence of O, S, Se, and Te.

s^2p^4. These atoms form stable glasses when alloyed with other elements such as Si, Ge, and As. And, in most of these glasses, the VIb atoms are two-fold coordinated, with some exceptions of higher coordination numbers in Te-glasses, probably reflecting metallic character of heavy atoms, and in ion-conducting chalcogenide glasses such as Ag-As-S. Neglecting these exceptions, we can regard that short-range structures of group-VIb covalent (partially, ionic) glasses are topologically the same. And, these two-fold coordinated atoms produce qualitatively the same electronic structures. The valence band is composed by lone-pair p-electron states, σ bonding states lying lower in energy, and the conduction band is composed by σ^* anti-bonding states.

However, there exist notable differences among the four atoms[9]. As shown in Fig. 1, E_g and the network dimensions are substantially different. In addition, reflecting the medium-range structures, glass-transition temperatures T_g of the chalcogenide (250 - 500 K) and the oxide (500 - 1500 K) are fairly different. Also, as is known, these glasses have very different historical backgrounds. Artificial oxide glasses were produced at the Mesopotamian age (~5000 years ago), while the chalcogenide has been utilized at most in these ~50 years. It is therefore interesting to start with a comparison of historical backgrounds of photoinduced phenomena in the oxide and the chalcogenide glass.

3. Historical

Since the optical gap of oxide glasses is wider than

~5 eV, we naturally assume that only high-energy photons of UV light, x-ray, and γ-ray are capable of producing some photoinduced effects. The effects are, in general, creation of defects appearing as color-centers, which are easily noticed in originally-transparent glasses. Accordingly, optical and ESR properties have been studied in this half century[4,19]. For instance, the famous E' center was reported by Weeks in 1956[20]. On the other hand, in the 60's, Primak and Kampwirth discovered a macroscopic irradiation effect, the so-called radiation compaction, in SiO_2[21]. These pioneering studies appear to correlate with the advent of nuclear technology.

More recently, production of high-purity optical fibers and new lasers stimulates application-oriented studies. Hill et al. discovered using Ar-ion lasers a photoinduced refractive-index increase in Ge-doped SiO_2 glass[22], which has triggered extensive developments of photonics-glass devices such as Bragg-reflector fibers[23]. In addition, studies using pulsed lasers with fs - ns durations are becoming common[15,24]. Pulsed light is likely to excite mid-gap states and/or to trigger multi-photon processes, which can provide micro-machining and drilling.

On the other hand, world-wide studies on photoinduced phenomena in chalcogenide glasses began at ~1970. Berkes et al.[25] and deNeufville et al.[26] reported comprehensive results on photostructural changes in $As_2S(Se)_3$ films. For telluride films, Ovshinsky's group discovered opto-thermal structural changes between crystalline and amorphous states[27], which have now been commercialized as erasable DVDs (digital versatile disks). Photodoping of Ag into sulfide glasses, discovered by Kostyshin et al.[28], has attracted renewed interest in photolithography also since 70's[29,30].

4. Photo-excitation and Structural Changes

As shown in Fig. 3, light illumination gives three effects, which are photo-electronic, thermal, and plasma-induced. The photo-electronic effect appears upon weak light (limited-dose) illumination. When absorbed light power is greater than ~1 kW/cm³, continuous and pulsed light can provide thermal and nonlinear effects (see, Fig. 4).

Table 1 classifies a variety of non-thermal photoinduced phenomena with typical recovering times. The phenomena can be characterized in two ways. On one

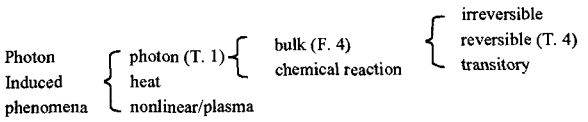

Fig. 3. Classification of photoinduced phenomena in simple oxide and chalcogenide glasses. (···) shows related figures and tables.

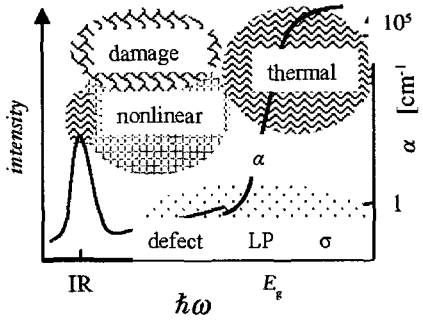

Fig. 4. Spectrum-intensity dependences of electronic, thermal, and nonlinear effects, and damage. As shown above the horizontal axis, the electronic effect may occur through excitations of defects, lone-pair electrons (LP), and σ electrons. A typical absorption spectrum α is shown with the right-hand axis.

Table 1. A classification of non-thermal photoinduced phenomena. Δα, Δn, ΔV, and Δη represent changes in optical absorption, refractive index, volume, and viscosity. PSD is for photo-surface deposition, PD for photodarkening, MGA for mid-gap absorption, and PCM for photo-chemical modification.

mode (recovery time)	bulk change	chemical reaction
Irreversible (∞)	crystallization, polymerization, ΔV	oxidation, photodope, PSD
reversible (min)	PD, Δn, ΔV, MGA & ESR	PCM
transitory (ms - s)	Δα, Δn, ΔV, Δη	

hand, the phenomena can be divided into bulk changes (Fig. 5) and photo-chemical reactions. The bulk change occurs in single phases, while two materials may react *photo-chemically*. On the other hand, these phenomena can be characterized by recovering time as follows:

Some photoinduced changes are *irreversible*, that is, un-recoverable by any means. Known examples are photo-crystallization in a-Se[31] and photo-polymerization in as-evaporated molecular As_2S_3 films[26], which resembles that in organic photoresists. Photodoping[29] and photo-surface deposition (PSD)[30], the both being related with Ag migration, are also irreversible. As illustrated in Fig. 5, irreversible changes occur reflecting

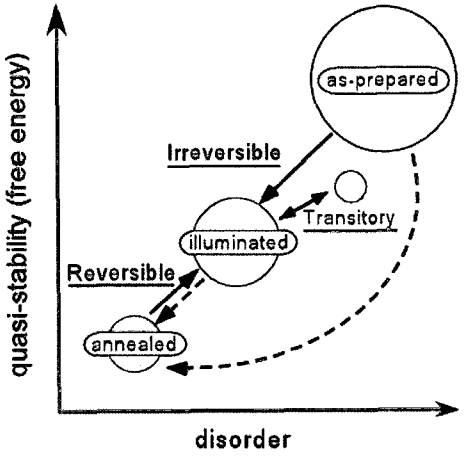

Fig. 5. Bulk changes of irreversible, reversible, and transitory processes between as-prepared (as-evaporated), illuminated, annealed, and under-illumination states. Dashed lines depict relaxational changes induced by annealing.

non-stability of initial states.

Reversibility can be obtained by annealing treatments of min - h durations. For photodarkening (PD) the annealing should be done at glass-transition temperatures T_g[26], while for photoinduced mid-gap absorption (MGA) and electron-spin resonance (ESR) signals a needed temperature is at ~ $T_g/2$[10]. Note that, as illustrated in Fig. 5, in many cases, as-prepared samples after direct illumination (irreversible) and after annealing-illumination treatments (reversible) have similar properties of the illuminated state. Another reversible process, which may be less common, is the photo-chemical modification (PCM) in Ag-As-S glasses[30], in which Ag concentration can be reversibly modified by changing illuminated regions.

Lastly, a change can be referred to as *transitory*, if it appears only under illumination and disappears at the cessation with time constants of ms - min. Photochromic effects in oxide glasses have long been known, and similar optical changes are discovered for chalcogenide glasses[32-35]. Transitory optical changes appear also in liquid S and Se[36]. These transitory changes may become quasi-stable (reversible) when illumination is provided at lower temperatures. In addition, under illumination, volume and viscosity appear to, respectively, expand[37] and decrease[38-43]. However, sample temperature necessary rises under illumination, and accordingly, resulting effects such as thermal expansion should be carefully evaluated.

Furthermore, these three kinds of changes may reflect polarization of illuminating light, in which cases the change becomes *anisotropic* (see, Fig. 9)[44-47]. A prominent change is a polarization-dependent transitory opto-mechanical effect, which appears as bending of bi-layer structures consisting of a chalcogenide film and a thin substrate[48,49].

Here, it may be valuable to mention the followings: First, for instance, in evaporated As_2S_3 films, magnitudes of the changes, e.g., in refractive index Δn for illumination at room temperature are "irreversible (~0.13) > reversible (~0.02) > transitory (~0.003) ≈ anisotropic (~0.001)". Second, we should note that, even for single materials, photoinduced effects are likely to be different in samples prepared in different ways. An example can be pointed out in recent studies for GeO_2 film[50] and glass[51]. Third, following the classification based upon the response time, we can assume that nonlinear optical phenomena appearing with sub-ps response times, such as two-photon absorption, are also kinds of photoinduced phenomena. However, only photoinduced changes in nonlinearity will be mentioned in this article.

Table 2 shows a sequential photoinduced process with related variables and modifications. Notable features are described below.

4.1. Exposure and Excitation

Light exposures have a variety of parameters such as photon energy $\hbar\omega$, irradiance, polarization, and so forth.

Table 2. An energy flow in photoinduced phenomena with typical features

light →	*excitation* →	*structural change* →	*property modification*
cw/pulse	electronic	chemical/ionic reaction	density (volume/shape)
photon energy	electro-thermal	atomic change	thermal/mechanical
irradiance	thermal	normal bonding	optical
polarization	plasma	defective	electrical
focusing		sputtering/explosion	chemical
temperature			surface property

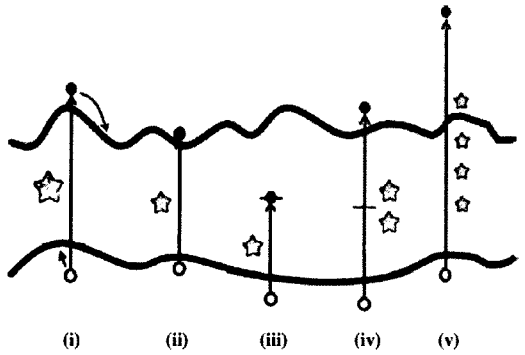

Fig. 6. Several photo-electronic excitations through (i) one-photon bandgap, (ii) one-photon sub-gap, (iii) one-photon half-gap, (iv) resonant two-photon, and (v) multi-photon processes in glasses. The size of stars depicts related photon energy.

Electronic excitation is indispensable for photo-structural changes. Super-gap ($\hbar\omega > E_g$) illumination (Fig. 6i) may excite σ bonding electrons, which are located energetically lower than the valence band. Accordingly, the excitation is likely to provide bond breaking and interchanges, as listed in Table 3. Bandgap ($\hbar\omega \approx E_g$) and sub-gap (Urbach-edge light with $\hbar\omega \lesssim E_g$) illumination (Fig. 6ii) can excite lone-pair electrons in the valence band[40,52], providing a variety of structural changes. Mid-gap light ($\hbar\omega \approx E_g/2$) can excite defects (Fig. 6iii), and if it is pulsed with high peak irradiance (~1 GW/cm²), two-step and/or two-photon excitations (Fig. 6iv) occur[53]. More intense pulses may provide very non-linear multi-photon excitations (Fig. 6v) and plasma effects. Here, it should be emphasized that the low-energy photons have longer penetration depths of ~1 cm, so that these can produce volumetric effects, which are in marked contrast to surface-limited ($\lesssim$ 10 μm) effects by (super-)bandgap illumination.

Polarization adds further varieties. When light is unpolarized, only isotropic (scalar) photon-energy effects, which are electronic and/or thermal, can appear. On the other hand, linearly or circularly polarized light may exert electric-field effects, which are naturally non-thermal. Linearly-polarized light produces anisotropic (vector) changes[45,46,54], similar to the Weigert effect known in photographic science[55]. Anisotropic changes occur also when unpolarized light impinges obliquely or upon side surfaces of samples[45,46,56]. Illumination of intense linearly-polarized light may induce second-order optical nonlinearity, the process being referred to as *optical poling*[57,58]. Circular-polarized light seems to give gyrotropic changes, for which studies have been relatively limited[46].

Two additional factors are mentioned. When light is tightly focused to small spots, the exposure may give geometrical effects[59], boundary-stress effects[60,61], nonlinear effects[15,58,62], and so forth. Lastly, in chalcogenide glasses, the temperature T at which a sample is exposed to illumination is important, as mentioned above.

4.2. Structural Modifications

What changes are induced by illumination? The change is brought, at least, through three processes. First, excited electrons and holes may deform atomic structures through self-trapping, which correspond to polarons in insulating crystals, and then, the structure may be frozen-in after electron-hole recombination (photon mode). Second, in many cases, electrons and holes recombine non-radiatively, necessary rising sample temperature, which may govern successive structural changes if it is greater than ~100 K (heat mode). Lastly, if photo-electronic excitation is very intense, 1 GW/cm² - 1 TW/cm², electron-hole plasma may be formed[63,64], which can provide more violent effects appearing as spikes and damages. Such plasma processes seem to appear in crys-

Table 3. Comparisons of photoinduced phenomena as a function of excitation photon energy in SiO_2 and As_2S_3. Core-electron excitations are excluded. The bold parts represent many studies. 1P, 2P, and 2S denote one-photon, two-photon, and two-step

	SiO_2 ($E_g \simeq 9$ eV)	As_2S_3 ($E_g \simeq 2.4$ eV)
super-gap ($\hbar\omega > E_g$)	Si-Si, small ring	As-As, As_2O_3
Bandgap ($\hbar\omega \simeq E_g$)	Si-Si	**PD, $+\Delta V$, $+\Delta n$ (D^0 at low T)**
sub-gap ($\hbar\omega < E_g$)	**$-\Delta V$ and $+\Delta n$ by 7.9eV** 2S-excitation, E' centers and NBOHC by 2P-excitation	PD, + ΔV, + Δn by 2.0eV 1P-excitation
half-gap ($\hbar\omega \simeq E_g/2$)	**E', $-\Delta V$ and $+\Delta n$ by 6.4eV photons,** POR destruction by 5.0eV photons	1.2eV 1P-excitation gives no effects 2P excitation gives + Δn and As-As, but no PD

tals as well[65], i.e., the disorder is no more responsible for such intense excitations. The topic is, therefore, scarcely touched hereafter. These excitations induce a variety of structural changes (Table 1).

First, the chemical reaction includes oxidation[25,66], hydration[50,67], and Ag-related phenomena[28-30,68] such as photodoping. These changes arise from gross bonding changes, which are relatively easy to detect and analyze. Photo-reduction of rare-earth ions may be regarded as a chemical reaction[15,62].

Second, the bulk change occurs in normal-bonding and defective structures. The most prominent change may be irreversible giant photo-contractions in volume

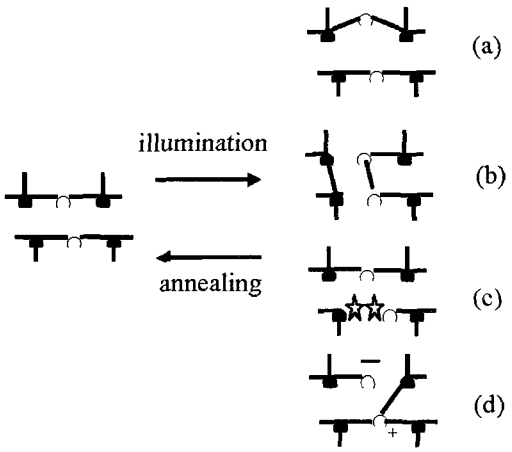

Fig. 7. Models for bulk reversible (transitory) photoinduced changes; (a) normal-bonding disordering and creations of (b) wrong bond, (c) neutral dangling bond D^0 (including E' and etc), and (d) charged defects, D^+ and D^-. Open circles are oxygen or chalcogen atoms and closed circles are As, which may be replaced to Si or Ge, and a star represents an unpaired electron.

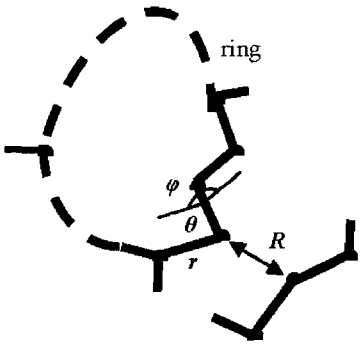

Fig. 8. Bond distance r, bond angle θ, dihedral angle φ, and inter-molecular distance *R*, and a ring structure.

of ~30 % observed in obliquely-deposited Ge-Se films[69], which arise from micro-voids collapsing with illumination. Nevertheless, many bulk changes are subtle and difficult to identify as describe in the followings:

The normal-bonding structural change includes polymerization[26], decomposition[25], amorphization[27], crystallization[31,70], and disorder increases. The last one (Fig. 7a) is the most problematic due to many possibilities of disordering elements (see, Fig. 8); e.g., covalent-bond distance r, bond angle θ, dihedral angle φ, intermolecular distance R, and ring static. These structural changes can be probed directly using x-rays (diffraction and absorption spectroscopy) and vibrational spectroscopy[10,26,41,71]. However, identifications of detected modifications are difficult, because prominent signatures such as x-ray first-sharp diffraction peak (FSDP) and Raman-scattering Boson-peak themselves remain to be un-identified[72-76]. Therefore, elucidation of photoinduced disordering elements is not straightforward. A transitory disordering increase is also detected in samples under illumination, but the interpretation can neither be explicit[77].

On the other hand, the defective change includes creation of wrong bonds (homo-polar bonds in stoichiometric glasses) and dangling bonds. If the defect density is ~1 at%, as for the case of As-As bonds in As_2S_3 (Fig. 7b), we can detect them using Raman-scattering spectroscopy and identify the structure more-or-less convincingly. For a less-dense defect, if it has unpaired electrons (Fig. 7c) it can be detected through ESR with sensitivity of ~10^{15} cm^{-3}, examples being E' centers (≡Si ·), NBOHC (non-bridging oxygen hole center; ≡Si-O ·), and POR (per-oxy radical; ≡Si-O-O ·) in SiO_2 and neutral dangling bond D^0 in the chalcogenide. The resonance line-shapes may be analyzed for obtaining structural insights. However, it is difficult to identify sparse defective structures having paired electrons (Fig. 7d); e.g. ODC (oxygen-deficient center, Si wrong bond, ≡Si-Si≡) and positively and negatively charged-dangling bonds, D^+ and D^-[10,78-80]. In such cases, more indirectly, optical absorption and photoluminescence spectroscopy may provide some information on defects if these have unique electronic states. Such optical methods are pertinent specifically to oxide glasses since these have wide optical gaps. However, for chalcogenide glasses, origins of weak absorption tails and photolu-

minescence are still vague[81-83], and accordingly, it is difficult to interpret explicitly photoinduced optical modifications.

Anisotropic and chiral structures in disordered materials are in general more difficult to detect. And, only a few structural studies on the photoinduced change have been reported[45,46,84]. Exceptional is anisotropic (oriented) crystallization in Se, which has been confirmed using x-ray diffraction[85] and Raman scattering[86].

4.3. Property Modifications

The simplest photoinduced change may be a volume change (ΔV in Table 4). The change appears as an expansion in As_2S_3[59,87] and a depression in SiO_2[4,21]. The expansion can be regarded as a kind of Shottky-defect formations, and the depression appears as compaction of less-dense structures[88]. As shown in Fig. 9, anisotropic deformations also appear upon illumination of linearly-polarized light[89], the mechanism being studied[90].

Structural properties such as thermal and mechanical are also modified. Glass-transition behaviors manifest that the illuminated state is quasi-stable in comparison to the fully-annealed state[91,92]. Irreversible and reversible changes in elastic constants are induced in

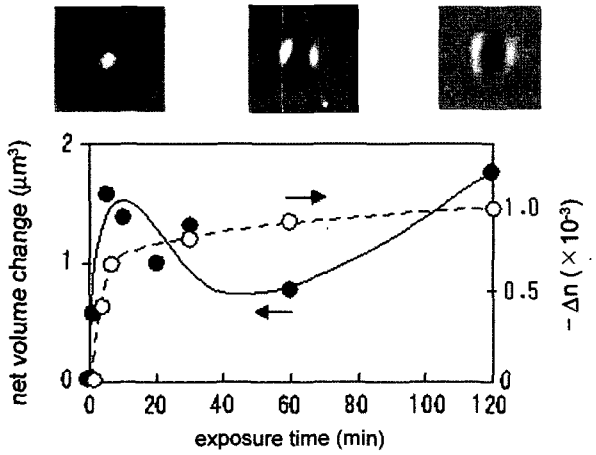

Fig. 9. Exposure-time dependence of volume change (solid line) and birefringence (dashed line) in an annealed As_2S_3 film exposed to linearly-polarized light with photon energy of 2.0 eV, intensity of 2 mW, and spot diameter of ~10 μm[90]. The upper three photographs show AFM profiles of illuminated area at exposure times of 1, 60, and 120 min, in which the polarization axis is horizontal. An exposure of 1 min produces a simple expansion with a diameter determined by the light spot, while it changes to M-shaped cross sections at 60 and 120 min.

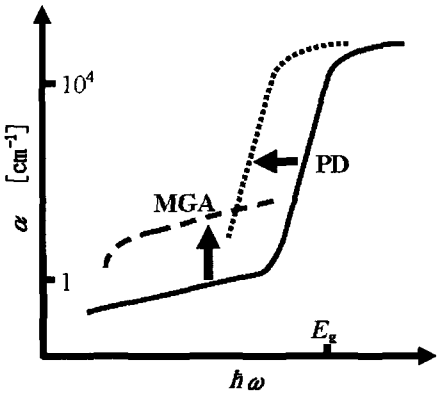

Fig. 10. Photodarkening (PD) and mid-gap absorption (MGA).

As_2S_3 when exposed to bandgap illumination[93,94]. Subgap illumination gives rise to transitory fluidity[39,40,95,96], which can produce permanent shape changes in As_2S_3 flakes[40,59]. Such electronic fluidity cannot be detected in Pyrex glasses and polyethylene sheets, which implies that low-dimensional chalcogenide structures are essential to the phenomenon. Probably related with the photoinduced fluidity is a photoinduced change in microhardness in As-Se films continually studied by Trunov[43,97].

Optical changes in absorption and refractive index have been studied in details, probably because the change can be detected with high sensitivity and it may be applied to some devices:

Among several optical absorption changes, studies on the two phenomena are extensive, which are photoinduced mid-gap (defective) absorption and photodarkening, schematically illustrated in Fig. 10. The photodarkening, which refers to a photoinduced red-shift of optical absorption edges, is inherent to covalent chalcogenide glasses when exposed to (sub-)bandgap light with irradiance of ~50 mW/cm² for durations of min. Not only alloys but pure S[98] and Se[99,100] films show photodarkening. By contrast, I do not know convincing reports on the photodarkening in oxide glasses[101]. Ionic chalcogenide glasses such as Na_2S-GeS_2 appear not to exhibit photodarkening[102]. On the other hand, photoinduced mid-gap absorption[10,81,103,104] appears in both the oxide and the chalcogenide (at low temperatures).

Refractive index increases in response to two processes. It increases with the photodarkening, which can

be understood on the basis of the Kramers-Krönig relation. In terms of the Lorentz-Lorenz relation, $(n^2-1)/(n^2+2) = N\gamma/(3\varepsilon_0)$ (where, N is the density of dipoles, γ the polarizability, and ε_0 the dielectric constant in vacuum), the photodarkening is assumed to be a manifestation of an increase in γ. On the other hand, the photoinduced refractive-index increase in (Ge-)SiO_2 can be related to the volume compaction[4], which gives rise to an increase in N. Here, Ge atoms in SiO_2 are assumed to act as sensitizers, while pure GeO_2 glass seems to undergo a different photoinduced change of bonding conversion from $GeO_{6/2}$ to $GeO_{4/2}$[51]. Effects of mid-gap absorption upon the refractive index change seem to be relatively small.

Photoinduced dichroism and birefringence (dashed line in Fig. 9), which are connected by the Kramers-Krönig relation, appears[44-46]. These vector changes are smaller by ~1/10 of the corresponding scalar changes, i.e. photodarkening and related refractive-index change, and accordingly, the vector had been assumed to be fractional effects of the scalar. However, some distinct characteristics such as light-intensity dependence and annealing kinetic manifest that their origins are different[45,46].

There are some less-commonly observed optical changes. Evaporated Ge-S films undergo irreversibly photobleaching, which arises from oxidation (GeO_2) and wrong-bond annihilation (≡Ge-Ge≡ → ≡Ge-S-Ge≡)[106]. The photo-polymerization in evaporated $As_2S(Se)_3$ films accompanies an irreversible red-shift of optical absorption edges[26]. Hajto et al. discovered a fascinating phenomenon, transmittance oscillation in $GeSe_2$ during illumination to He-Ne laser light, in which transmitted light oscillates in intensity with periods of ms - s[107].

Photoconductivity is also modified. It is generally suppressed by illumination[10], or exceptionally enhanced[108]. The suppression resembles that in a-Si:H, known as the Staebler-Wronski effect[109,110], the biggest problem for its application to solar cells. The photoconductivity suppression is ascribed in many cases to creation of dangling bonds, while the structures have not been elucidated. Lyubin et al. discovered that, after exposure to linearly-polarized light, photocurrents in $As_{50}Se_{50}$ films become anisotropic[46,111]. Chemical solubility changes upon illumination. Such solubility changes may be due to the polymerization, structural disordering, and oxidation. Surface-hydrophilicity also changes with illumination. Photoinduced change in surface reactivity of a-SiO_2 seems to be governed by defects[112].

Table 4. Comparison of reversible scalar photoinduced changes appearing in some materials at room temperature. X denotes non-existence. Typical data are given for As_2S_3[88], GeS_2 [unpublished], GeO_2[51,114], SiO_2[4,115], and a-Si:H[116,117]. Δn in a-Si:H may be too large.

	E_g [eV]	n	T_g [K]	$\Delta\alpha$	Δn	ΔV [%]
As_2S_3	2.4	2.6	450	PD	+0.02	+0.4
GeS_2	3.3	2.2	750	PD	+0.005	+0.5
GeO_2	5.8	1.6	850	MGA	$+10^{-4}$	+0.5
SiO_2	~9	1.5	1500	MGA	$+10^{-5}$	-10^{-3}
a-Si:H	~1.8	~3.2	x	MGA	-0.05?	$+10^{-3}$

Optical nonlinearity such as intensity-dependent refractive index n_2 and two-photon absorption coefficient β may be modified through prominent photostructural changes[58,113]. However, studies on the mechanisms remain.

5. Models and Problems

It is instructive to delineate overall processes of a photoinduced change by using energy-configuration (E-q) diagrams (see, Table 5)[1,2]. Here, the horizontal axis represents or signifies $3N$-6 atomic configurations (N being the atomic number), and accordingly, it is in general multi-dimensional[118]. The vertical energy is the summation of electronic and atomic systems at 0 K, i.e., the so-called adiabatic potential. Accordingly, the Franck-Condon principle postulates that an optical transition occurs as a vertical line, and a lattice relaxation is depicted as a transversal lowering. In such diagrams, as illustrated in Table 5, irreversible and reversible changes can be grasped using energy-configuration curves having asymmetric double-well ground-state potentials, in which the photo-produced configuration is stable and quasi-stable, respectively. As shown by a dashed arrow, the quasi-stable state can be annealed to the initial state. On the other hand, the photo-excited state may have a single well.

Table 5 suggests that the irreversibility and reversibility have some correlations with related atomic densities and extending spatial scales. The irreversible change

Table 5. Irreversible and reversible photoinduced changes in chalcogenide, oxide, and a-Si:H with configuration diagrams, related (estimated) atomic density and structural extension. Wavy and dashed arrows in the diagrams denote optical excitations and thermal annealing. LR and MR denote long- (> 10 nm) and medium-range (0.5–2 nm) extensions

Reversibility	Structural change (atom density)	Materials		
		chalcogenide	oxide	a-Si:H
Irreversible 	LR $\sim 10^{22}$ [cm^{-1}]	*crystallization giant contraction polymerization decomposition*	*decomposition*	*crystallization*
Reversible 	MR $\sim 10^{20}$	*darkening anisotropy*		
	defect $10^{16\sim17}$	*MGA & ESR*	*MGA & ESR*	*S-W effect*

such as polymerization and crystallization seems to accompany structural changes of ~1/5 atoms, which occur over long-range (LR) scales. This observation implies that an energy relaxation of overall structures causes the irreversibility. On the other hand, the reversible change occurs in medium-range (MR)orders or in defective structures with related atomic densities smaller than ~1 %. Such localized disordered structures should be energetically quasi-stable and can be annealed out. It seems that the participation of ~1% atoms divides the irreversible and the reversible. This is the reason why the reversible change is smaller than the irreversible. Note that short-range structures (< 0.5 nm) in normal bonding networks remain mostly intact due to rigidities.

Among many photoinduced phenomena, the most controversial but scientifically interesting and technologically promising may be the bulk thermally-reversible disorder enhancement. Several structural models have been proposed, which are divided into the two kinds. One is the modification in medium-range normal-bonding structures (Fig. 7a), which appear to cause the photodarkening in $As_2S(Se)_3$ and $GeS(Se)_2$ at room temperature[10,98]. The other is the defective-structure creation (Fig. 7b, c, and d), which may be dominant in SiO_2[4,10,19,120] and also in a-Si:H[10,110]: Photoinduced dangling-bond creation (MGA) observed in $As_2S(Se)_3$ at low temperatures ($\lesssim$ 100 K)[10,81] is also a defective process. These observations suggest that the defect creation is inherent to rigid and/or thermally un-relaxed structures. Interestingly, the densities of photoinduced defects are commonly $10^{16\sim17}$ cm^{-3} in these three materials, but how can we interpret this coincidence?[119]. In addition, for these phenomena, many problems remain unresolved as exemplified in the followings:

For SiO_2, unclear is a relationship between the photoinduced defect creation and volume compaction[4,122]. Since the number (~10^{15} cm^{-3}) of E' centers, estimated from ESR signals and optical absorption, cannot quantitatively explain the macroscopic volume compaction of 10^{-5} in fraction (Table 4), which may correspond to the atomic number of 10^{17} cm^{-3}, we should envisage some ingenious mechanisms. Takahashi et al.[123] proposes that the defect works as a catalytic element for the volume compaction. Nevertheless, the photoinduced behavior is known to depend upon quality (stoichiometry and impurity) of SiO_2 glass[123,124], and accordingly, the mechanism seems to be more complicated.

For the photodarkening, a lot of studies have been done[10], while it is fair to conclude that related structural changes are not identified. This is because the structural change, which occurs in disordered structures, is subtle.

In addition, composition dependence remains puzzling. It has been known that the photodarkening becomes smaller with a sequence of "sulfide > selenide > telluride"[105], but why does the oxide not show the photodarkening (see, Fig. 11)[101] ? All these glasses have the valence band consisting of lone-pair electrons[9]. Hence, the absence of the photodarkening only in the

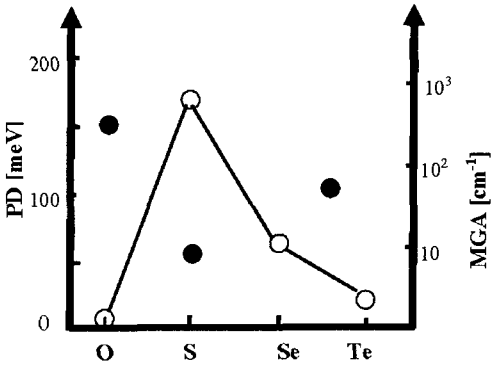

Fig. 11. Maximal photodarkening PD (○)[105] and mid-gap absorption MGA (●) in GeO_2[51] and $As_2S(Se\text{-}Te)_3$[81].

oxide glass should be sought in to more ionic bonds with large oxygen bonding angles of ~150°, smaller interaction between lone-pair electrons, and/or three-dimensional structures consisting of corner-sharing units of $SiO_{4/2}$. Which factor is the most responsible?

A speculation is as follows: Theoretical calculations show that the widths of lone-pair electron bands in crystalline SiO_2 and As_2Se_3 are ~4 eV[125] and ~6 eV[126], the magnitudes being consistent with the optical gaps of ~9 eV and ~2 eV. And, in SiO_2, σ* and σ bands are wider (~6 eV) than the lone-pair band, the situation being contrastive to that in As_2Se_3[9]. The narrower lone-pair band in SiO_2 implies smaller interaction between lone-pair electrons. Accordingly, the photodarkening, which is ascribed to a modification of lone-pair electron bands, may be undetectable in the oxide glass.

Another interesting problem is a relationship between the photodarkening and the photoexpansion. The both appear in, e.g., As_2S_3 when exposed to bandgap illumination, but with different growing time scales[88]. Then, what is the relation? My idea is that atomic disordering processes such as atomic twisting (Fig. 12), which cause the photodarkening, should be transferred to sample surfaces through photoinduced fluidity for appearing as macroscopic expansions[59]. That is, the origins are common, but the expansion needs transfer times through fluidity. On the other hand, Shimakawa et al. propose structural changes which are induced by electrical repulsion of photo-excited carriers[121].

Dynamics are more difficult to understand. Optical

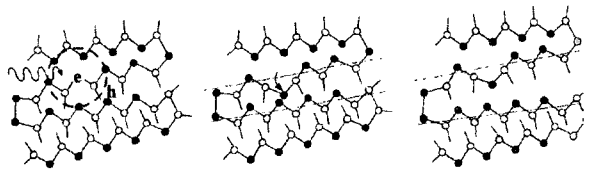

(a) (b) (c)

Fig. 12. A model for photo-expansion[40]. (a) A photon excites a pair of electron and hole. (b) When it is excited, the lattice undergoes a bond twisting due to de-stabilized intermolecular interaction. Nearly perpendicular bond-angles may be favorable to such motions. After this, the electron and hole may recombine. Through such processes, interaction between lone-pair electrons increases, which results in widening of the valence band, which appears as the photodarkening. (c) However, if the lattice is flexible, the inter-molecular stress may be relaxed with an inter-molecular expansion, which will be transferred to a sample surface, appearing as an observable expansion.

excitations using fs –ns lasers have been performed[24], but successive electro-structural processes are difficult to monitor due to disordered background structures. Note that, even for single crystals, such work has not been straightforward[1,2].

For these problems, computer simulations being carried out in several groups[127-131] provide valuable insights. However, the simulation contains unavoidable limitations such as anomalously-fast quenching rates for glass formation, small numbers of atoms, and neglect of photo-electronic excitation processes. The photo-excitation is simulated as putting an electron and a hole in conduction (LUMO) and valence (HOMO) bands in produced networks. Such treatments make incorporation of light-polarization effects difficult, and it has not been examined. In short, the computer simulation is able to suggest some possibilities, while real processes should be considered carefully.

6. Applications

Photoinduced effects can be applied to devices in three kinds of sample forms of fiber, film, and bulk. The fiber can provide long interaction distances over 1 m for propagating light, and accordingly, it is useful for utilizing small photoinduced changes in oxide glasses. For instance, we estimate a needed device length L as $L\Delta n = \lambda$, a condition for 2π phase-modulation of light waves, which gives L = 100 μm and 10 cm for $\Delta n = 10^{-2}$ and 10^{-5}. Accordingly, the fiber is required for conventional oxide glasses. On the other hand, light-propagation lengths in films and bulk samples ranges from a film thickness of ~100 nm to a lateral sample size of ~1 cm, and accordingly, these are useful to greater photoinduced changes in chalcogenide glasses[132,133] and some special oxides produced by sol-gel method[157] and so forth. Among several changes in macroscopic properties, the changes in reflectivity and refractive index have been utilized in optical devices.

Already commercialized are two devices. One is the erasable DVDs[27,134], which utilize reflectivity modifications upon optical heat-mode phase-changes in telluride films such as $Ge_2Sb_2Te_5$. The memory capacity in a recent blue-laser system is 50 GB/disk, in which a mark size is reduced to ~150 nm in diameter. The other is Bragg reflectors (phase grating) in Ge-doped

Table 6. Athermal photoinduced changes (ΔV, $\Delta\alpha$, Δn, and *Δetching*) and applications with some references

	ΔV	$\Delta\alpha$	Δn	*Δetching*
Imaging (holographic)			135-141	145
Grating	146,147		148-150	151-153
Waveguide			154-155	
Tuning			159-161	
Lens	162		162	162,163
Photonic crystal				164,165
Switch	49	154,166	167	

SiO_2 fibers utilizing refractive-index modifications, which are employed for wavelength divisions in optical communication networks[23]. In addition, there are many proposals of photoinduced devices as listed in Table 6.

For photon-mode optical memories, which may be holographic and three-dimensional, photoinduced refractive-index changes in sulfides and selenides have been studied for a long time[135-141]. However, such systems have not been commercialized. Why?

Will the photon-mode memory be compatible with the erasable DVD system? It seems that the possibility is small because of lower efficiencies. In a recent DVD, a phase change in ~150 nm spots is induced by a light pulse with a typical intensity and duration of 30 mW(~0.1 TW/cm^2) and 30 ns[134]. This corresponds to an energy of ~2 J/cm^2, which is ~ 10^{19} photons/cm^2, being 1 – 3 orders smaller than the photon number needed for the reversible photoinduced refractive-index change of 10^{-2} (Table 4). We need higher-power lasers for utilizing the erasable refractive-index change[142], but ~1 TW/cm^2 light is likely to damage chalcogenide films (Fig. 3). Such inefficiency in the index change is ascribable to less-unity quantum efficiency arising from isolated (non-cooperative) photostructural changes and thermal relaxation at room temperature. On the other hand, the heat-mode phase change utilizes thermally-assisted development processes including crystal growth and melting. Therefore, I believe that reversible photoelectronic changes are not suitable for erasable memories. Built-in (non-erasable) devices will be more promising.

Photoinduced changes ($\Delta\alpha$, Δn, ΔV, *Δetching*) in sulfides and selenides resulting from irreversible and reversible structural changes including photodoping[143,144] have been applied to many devices and purposes. Following Table 6, we may recall first that Sakai demonstrates copy masters using photo-etched surfaces[145]. Next, relief-type and phase gratings have been studied for a long time[146-153]. Since the chalcogenide glass has a high refractive index of 2 - 3, which gives high reflectance, Bragg gratings can be produced by single beams[40]. Third, applications to waveguides have been explored since 70's[154-158]. Recently, the waveguides are combined with optical nonlinear effects[153,156,158]. Fourth, photoinduced refractive-index changes have been applied to tuning of some parameters (wavelength, stability, etc.) in semiconductor devices such as laser diodes[159-161]. Fifth, micro-lenses, which can be cylindrical or aspherical, have been fabricated using the so-called giant-photoexpansion effect[59] and other techniques[162,163]. Three-dimensional photonic structures have been fabricated through illumination and etching[164,165], the technique being essentially the same with that for the copy master[145] but being more sophisticated.

Transitory changes may be useful for some applications operating with response times of ms – s. The absorption and refractive-index changes ($\Delta\alpha$, Δn) are promising to optical switches of waveguide types[154,166-168]. The transitory opto-mechanical effect[48] is also interesting in applications to micro-machines[49].

What is the future application? There seem to be two directions, which are related and unrelated with optical communication technologies. The related device must operate at wavelengths of ~1.5 μm, and it must be connected to oxide-glass fibers having refractive index of ~1.5. The most promising may be optical integrated circuits, in which passive elements can be produced using laser machining of oxide glasses. However, the oxide glass seems to be unsatisfactory for active elements such as all-optical switches using nonlinear effects. On the other hand, the chalcogenide device can have high fig-

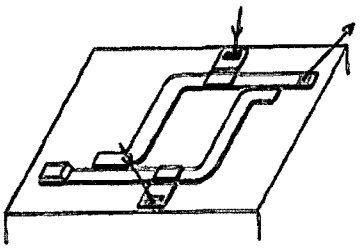

Fig. 13. A Mach-Zehnder interferometer type optical switch using photoinduced transitory refractive-index change[168].

ure-of-merits of the nonlinearity[132], which arise in principle from the smaller energy gap[58]. Therefore, further studies on integration will be valuable. However, some ideas for index-matching between the refractive indices of ~1.5 in the oxide and ~2.5 in the chalcogenide are needed. On the other hand, the unrelated are widespread, and the targets seem to be diverse as suggested in Table 6 and recent publications[169].

I would like to thank Dr. A. Saitoh and N. Terakado for reading and comments.

References

1. Y. Toyozawa, *Optical Processes in Solids* (Cambridge University Press, 2003).
2. N. Itoh and A.M. Stoneham, *Materials Modification by Electronic Excitation* (Cambridge University Press , 2001).
3. A.V. Kolobov (ed.), *Photo-Induced Metastability in Amorphous Semiconductors* (Wiley-VCH, 2003).
4. G. Pacchioni, L. Skuja, and D.L. Griscom (eds.), *Defects in SiO_2 and Related Dielectrics: Science and Technology* (NATO Science Series II, 2000).
5. O.U. Vonwiller, Nature 104 (1919) 347.
6. W. Primak, Phys. Rev. 110 (1958) 1240.
7. H. Hamanaka, K. Tanaka, and S. Iizima, Solid St. Commun. 23 (1977) 63.
8. T. Imura et al., J. Phys. Soc. Jpn. 52 (1983) 2459.
9. K. Tanaka, Optoelectronic Mater. Devices 1 (2004) 43.
10. K. Shimakawa, A. Kolobov, and S.R. Elliott, Adv. Phys. 44 (1995) 475.
11. H. Jain, J. Optelectronic Adv. Mater. 5 (2003) 5.
12. K. Tanaka, J. Non-Cryst. Solids 352 (2006) 2580.
13. R. Sramek et al., J. Non-Cryst. Solids 277 (2000) 39.
14. J. Heo and J.D. Mackenzie, J. Non-Cryst. Solids 111 (1989) 29.
15. K. Hirao et al., *Active Glass Devices*, (Springer, 2001).
16. M. Nogami et al., *Handbook of Advanced Electronic and Photonic Materials and Devices*, H.S. Nalwa (ed.) (Academic Press, 2001) Vol. 5, Chap. 5.
17. R. Zallen, *The Physics of Amorphous Solids*, (John Wiley & Sons, 1983).
18. K. Tanaka, *Encyclopedia of Materials: Science and Technology* (Elsevier, 2001) p. 1123.
19. L. Skuja et al., Proc. SPIE 4347, 155 (2001).
20. R.A. Weeks, J. Appl. Phys. 27 (1956) 1376.
21. W. Primak and R. Kampwirth, J. Appl. Phys. 39 (1968) 5651.
22. K.O. Hill et al., Appl. Phys. Lett. 32 (1978) 647.
23. A. Othonos and K. Kalli, *Handbook of Advanced Electronic and Photonic Materials and Devices*, H.S. Nalwa (ed.) (Academic Press, 2001) Vol. 9, Chap. 9.
24. K. Hirao and K. Miura, ibid. Ref. 3, Chap. 21.
25. J.S. Berkes, S.W. Ing, and W.J. Hillegas, J. Appl. Phys. 42 (1971) 4908.
26. J.P. DeNeufville, S.C. Moss, and S.R. Ovshinsky, J. Non-Cryst. Solids 13 (1973/74) 191
27. J. Feinleib et al., Appl. Phys. Lett. 18 (1971) 254.
28. M.T. Kostyshin, E.V. Mikhailovskaya, and P.F. Romanenko, Sov. Phys. Solid State, 8 (1966) 451.
29. T. Wagner and M. Frumar, ibid. Ref. 3, Chap. 10.
30. K. Kawaguchi, ibid. Ref. 3, Chap. 11.
31. J. Dresner and G.B. Stringfellow, J. Phys. Chem. Solids 29 (1968) 303.
32. A. Matsuda et al., Appl. Phys. Lett. 24 (1974) 314.
33. K. Tanaka and Y. Ohtsuka, J. Appl. Phys. 49 (1978) 6132.
34. M. Iijima and S. Kurita, J. Appl. Phys. 51 (1980) 2103.
35. A. Ganjoo and H. Jain, Phys. Rev. B 74 (2006) 24201.
36. Y. Sakaguchi and K. Tamura, ibid. Ref. 3, Chap. 12.
37. Y. Ikeda and K. Shimakawa, J. Non-Cryst. Solids 338-340 (2004) 539.
38. H. Koseki and A. Odajima, Jpn. J. Appl. Phys. 21 (1982) 424.
39. H. Hisakuni and K. Tanaka, Science 270 (1995) 974.
40. K. Tanaka, ibid. Ref. 3, Chap. 5.
41. S.N. Yannopoulos, ibid. Ref. 3, Chap. 8.
42. J. Gump et al., Phys. Rev. Lett. 92 (2004) 245501.
43. M.L. Trunov, J. Optpelectron. Adv. Mater. 7 (2005) 2235.
44. V.G. Zhdanov and V.K. Malinovskii, Sov. Tech. Phys. Lett. 3 (1977) 387.
45. K. Tanaka, *Handbook of Advanced Electronic and Photonic Materials and Devices*, H.S. Nalwa (ed.) (Academic Press, 2001) Vol. 5, Chap. 4.
46. V.M. Lyubin and M.L. Klebanov, ibid. Ref. 3, Chap. 6.
47. V.K. Tikhomirov et al., Appl. Phys. Lett. 84 (2004) 4263.
48. P. Krecmer et al., Science 277 (1997) 1799.
49. M. Stuchlik, P. Krecmer, and S.R. Elliott, ibid. Ref. 3, Chap. 7.
50. N. Terakado and K. Tanaka, J. Non-Cryst. Solids 351 (2005) 54.
51. N. Terakado and K. Tanaka, J. Non-Cryst. Solids 352 (2006) 3815.
52. H. Hosono et al., Phys Rev. Lett. 87 (2001) 175501.

53. K. Tanaka, Philos. Mag. Lett. 84 (2004) 601.
54. V.R. Bhardwaj et al., Phys. Rev. Lett. 96 (2006) 57404.
55. F. Weigert, Ann. Phys. 63 (1920) 681.
56. K. Tanaka et al., Solid St. Commun. 95 (1995) 461.
57. A.J. Ikushima et al., J. Appl. Phys. 88 (2000) 1201.
58. K. Tanaka, J. Mater. Sci.: Mater. Electron. 16 (2005) 633.
59. K. Tanaka, A. Saitoh, and N. Terakado, J. Optoelectron. Adv. Mater. 8 (2006) 2058.
60. M. Nakamura et al., J. Non-Cryst. Solids 198-200 (1996) 740.
61. T. Honma et al., Appl. Phys. Lett. 88 (2006) 231105.
62. K. Hirao and K. Miura, ibid. Ref. 3, Chap. 21.
63. A. Salleo et al., Nature Mater. 2 (2003) 796.
64. A.Q. Wu et al., Appl. Phys. Lett. 88 (2006) 111502.
65. S. Juodkazis et al., Phys. Rev. Lett. 96 (2006) 166101.
66. K. Ogusu et al., J. Non-Cryst. Solids 351 (2005) 3132.
67. K. Tanaka, N. Nemoto, and H. Nasu, Jpn. J. Appl. Phys. 42 (2003) 6748.
68. T. Kawaguchi, K. Tanaka, and S.R. Elliott, *Handbook of Advanced Electronic and Photonic Materials and Devices*, H.S. Nalwa (ed.) (Academic Press, 2001) Vol. 5, Chap. 3.
69. A. Kumar et al., J. Appl. Phys. 65 (1989) 1671.
70. K. Sakai et al., J. Non-Cryst. Solids 320 (2003) 223.
71. C. Guillon et al., Appl. Phys. Lett. 89 (2006) 251913.
72. P.S. Salmon et al., Nature 435 (2005) 75.
73. J. Du and R. Corrales, Phys. Rev. B 72 (2005) 92201.
74. E. Bychkov, C.J. Benmore, and D.L. Price, Phys. Rev. B72 (2005) 172107.
75. A. Monaco et al., Phys. Rev. Lett. 96 (2006) 205502.
76. B.K. Sharma and M. Wilson, Phys. Rev. B 73 (2006) 60201.
77. A.V. Kolobov et al., Phys. Rev. B 55 (1997) 726.
78. D. Mao et al., Phys. Rev. B 48 (1993) 4428.
79. M. Seki et al., J. Non-Cryst. Solids 324 (2003) 127.
80. N.A. Bhat et al., J. Non-Cryst. Solids 319 (2003) 192.
81. R.A. Street, Adv. Phys. 25 (1976) 397.
82. C.M. Gee and M. Kastner, J. Non-Cryst. Solids 40 (1980) 577.
83. K. Tanaka et al., J. Appl. Phys. 91 (2002) 125.
84. G. Chen et al., Appl. Phys. Lett. 82 (2003) 706.
85. K. Ishida and K. Tanaka, Phys. Rev. B 56 (1997) 206.
86. V.V. Poborchii et al., Appl. Phys. Lett. 72 (1998) 1167.
87. H. Hamanaka et al., Solid St. Commun. 19 (1976) 499.
88. K. Tanaka, Phys. Rev. B 57 (1998) 5163.
89. A. Saliminia et al., Phys. Rev. Lett. 85 (2000) 4112.
90. K. Tanaka and H. Asao, Jpn. J. Appl. Phys. 45 (2006) 1668.
91. B.T. Kolomiets et al., Sov. Phys. Solid State 21 (1979) 594:
92. P. Lucas et al., Phys. Rev. B 71 (2005) 104207.
93. K. Tanaka et al., Jpn. J. Appl. Phys. 20 (1981) L874.
94. J. Honolak, G. Kasper, and S. Hunklinger, Europhys. Lett. 57 (2002) 382.
95. K. Tanaka, C.R. Chimie 5 (2002) 805.
96. J. Gump et al., Phys. Rev. Lett. 92 (2004) 245501.
97. M.L. Trunov, S.N. Dub, and R.S. Shmegera, Solid St. Phenomena 115 (2006) 245.
98. K. Tanaka, Jpn. J. Appl. Phys. 25 (1986) 779.
99. K. Tanaka and A. Odajima, Solid St. Commun. 43 (1982) 961.
100. A. Reznik et al., J. Non-Cryst. Solids 352 (2006) 1595.
101. N. Terakado and K. Tanaka, Jpn. J. Appl. Phys. 46 (2007) 1265.
102. V.K. Tokhomirov et al., Appl. Phys. Lett. 71 (1997) 2740.
103. S.G. Bishop et al., Phys. Rev. Lett. 34 (1975) 1346.
104. J. Hautala, W.D. Ohlsen, and P.C. Taylor, Phys. Rev. B 38 (1988) 11048.
105. K. Tanaka, J. Non-Cryst. Solid 59&60 (1983) 925.
106. K. Tanaka, Y. Kasanuki, and A. Odajima, Thin Solid Films 117 (1984) 251.
107. J. Hajto and I. Janossy, ibid. Ref. 3, Chap. 9.
108. N. Toyosawa and K. Tanaka, Phys. Rev. B 56 (1997) 7416.
109. D.L. Staebler and C.R. Wronski, J. Appl. Phys. 51 (1980) 3262.
110. P. Stradins and M. Kondo, ibid. Ref. 3, Chap. 13.
111. V. Lyubin et al., Phys. Rev. Lett. 87 (2001) 216806.
112. C.-L. Kuo and G.S. Hwang, Phys. Rev. Lett. 97 (2006) 66101.
113. H. Xiang et al., Opt. Mater. 28 (2006) 1020.
114. Y. Watanabe et al., J. Non-Cryst. Solids 239 (1998) 104.
115. R.E. Schenker and W.G. Oldham, J. Appl. Phys. 82 (1997) 1065.
116. N. Souffi et al., Solid St. Commun. 122 (2002) 259.
117. S. Nonomura, ibid. Ref. 3, Chap. 14.
118. In the simplest case of single H_2 molecules, it is one-dimensional.
119. K. Tanaka, J. Non-Cryst. Solids 139 (1992) 179.
120. P. Lucas, J. Phys. Condens. Mater. 18 (2006) 5629.
121. K. Shimakawa et al., Philos. Mag. Lett. 77 (1998)

153.
122. K. Awazu and H. Kawazoe, J. Appl. Phys. 94 (2003) 6243.
123. M. Takahashi et al., J. Am. Ceram. Soc. 85 (2002) 1089.
124. Y. Ikuta et al., Appl. Opt. 43 (2004) 2332.
125. M.-Z. Huang et al., Phys. Rev. B 59 (1999) 3540.
126. E. Tarnow et al., Phys. Rev. B 34 (1986) 4059.
127. T. Uchino et al., Phys. Rev. B 65 (2002) 174204.
128. D.A. Drabold et al., ibid. Ref. 3, Chap. 15.
129. S.I. Simdyankin et al., Phys. Rev. Lett. 94 (2005) 86401.
130. J. Hegedus et al., Phys. Rev. Lett. 95 (2005) 206803.
131. M. Boero et al., Appl. Phys. Lett. 86 (2005) 201910.
132. K. Richardson et al., ibid. Ref. 3, Chap. 23.
133 A. Zakery and S.R. Elliott, J. Non-Cryst. Solids 330 (2003) 1.
134. T. Ohta and S.R. Ovshinsky, ibid. Ref. 3, Chap. 18.
135. S.A. Keneman, Appl. Phys. Lett. 19 (1971) 205:
136. V.I. Mandrosov et al., Opt. Spectrosc. 35 (1973) 75.
137. S. Zembutsu et al., Appl. Opt. 14 (1975) 3073.
138. S. Zembutsu and S. Fukunishi, Appl. Opt. 18 (1979) 393.
139. J.M. Gonzalez-Leal et al., ibid. Ref. 3, Chap. 20.
140. A. Ozols and M. Reinfelde, J. Opt. A: Appl. Opt. 6 (2004) S134.
141. S. Sainov et al., Opt. Commun. 263 (2006) 163.
142. K. Tanaka, J. Appl. Phys. 65 (1989) 2042.
143. M. Frumar and T. Wagner, Curr. Opinion Sol. St. Mater. Sci. 7 (2003) 117.
144. P.J.S. Ewen, ibid. Ref. 3, Chap. 22.
145. T. Sakai, Opt. Commun. 24 (1978) 47.
146. S. Ramachandran et al., IEEE Photonics Technol. Lett. 8 (1996) 1041.
147. J. Tetris and M. Reinfelde, J. Optpelectron. Adv. Mater. 7 (2005) 2581.
148. S. Zembutsu et al., Appl. Opt. 19 (1980) 937.
149. R. Vallee et al., Opt. Commun. 230 (2004) 301
150. M. Shokooh-Saremi et al., J. Opt. Soc. Am. B23 (2006) 1323
151. T. Glaser et al., Electron. Lett. 40 (2004) 176.
152. S. Noach et al., Opt. Mater. 28 (2006) 1054.
153. T. Clement et al., Opt. Express 14 (2006) 1789.
154. A. Matsuda et al., Appl. Opt. 13 (1974) 1992.
155. A. Zoubir et al., Opt. Lett. 29 (2004) 748.
156. Ramachandran and S.G. Bishop, IEEE J. Select Topics Quantum Electron. 11 (2005) 260.
157. R.K. Pita et al., Appl. Phys. Lett. 89 (2006) 71105.
158. G. Nunzi Conti et al., Appl. Phys. Lett. 89 (2006) 121102.
159. O. Mikami et al., Appl. Phys. Lett. 31 (1977) 376.
160. T.K. Sudoh et al., Electron. Lett. 33 (1997) 216.
161. S. Song et al., Appl. Phys. Lett. 89 (2006) 41115.
162. D. Savastru, S. Miclos, and R. Savastru, J. Optoelectron. Adv. Mater. 8 (2006) 1165.
163. N.P. Eisenberg et al., J. Non-Cryst. Solids 352 (2006) 1632.
164. A. Feigel et al., Appl. Phys. Lett. 83 (2003) 4480.
165. S. Wong et al., Adv. Mater. 18 (2006) 265.
166. L.E. Zou et al., Appl. Phys. Lett. 88 (2006) 153510.
167. K. Tanaka et al., J. Appl. Phys. 57 (1985) 4897.
168. Y. Imai et al., Opt. Quantum Electron. 17 (1985) 119.
169. W. Liang et al., Appl. Phys. Lett. 86 (2005) 151122.